5th Joint International Symposium on Deformation Monitoring (JISDM), 20-22 June 2022, Valencia, Spain
DOI: http://doi.org/10.4995/JISDM2022.2022.13729

Assessing sandy beach width variations on intertidal time scales using permanent laser scanning

Mieke Kuschnerus[1], Roderik Lindenbergh[1], Sierd de Vries[2]

[1] Department of Geoscience and Remote Sensing, Delft University of Technology, Stevinweg 1, 2628 CN Delft, The Netherlands, (m.kuschnerus@tudelft.nl; r.c.lindenbergh@tudelft.nl)
[2] Department of Hydraulic Engineering, Delft University of Technology, Stevinweg 1, 2628 CN Delft, The Netherlands, (sierd.devries@tudelft.nl)

Key words: *permanent laser scanning; long term monitoring; coastal deformation; change detection*

ABSTRACT

Coastal zones are highly dynamic, and their topography is subject to constant deformation. These deformations are governed by sediment transports that are forced by environmental conditions of waves, tides and wind which result in topographic changes at various spatial and temporal scales. In the view of climate change and intensification of extreme weather events, it is important for coastal management to monitor the deformation and coastal topography with high accuracy. To demonstrate a novel way of deriving these deformations and of analyzing the underlying processes, we use permanent laser scanning (PLS) to monitor part of the typical urban coastal beach in Noordwijk, The Netherlands. A laser scanner permanently installed on a hotel building acquired one 3D point cloud of the sandy beach and dunes every hour, continuously, for a duration of two years. The resulting spatio-temporal data set consists of ~ 15 000 point clouds and contains the evolution of a section of the coast of ~ 1 km length at great detail. The elevation changes are observed at centimeter level, allowing to monitor even small scale and slow processes. However, this information is not readily available from the extensive data set. By deriving digital elevation models (DEMs) from each point cloud and collecting elevation data as time series per spatial grid cell, we structure the data in an efficient way. We use the DEMs to estimate two parameters describing the coastal deformation, beach width and intertidal width. We also extract the shoreline at low and high tide for a part of the data set and estimate beach width and intertidal width from them. We find that heavy storms influence the location of the shoreline and the intertidal width in particular. Ultimately, the estimated beach width and intertidal width at high temporal frequency (monthly) and with high spatial accuracy (meters) helps coastal management to improve the understanding of coastal deformation processes.

I. Introduction

A. *Background*

Sandy coasts are very dynamic areas, undergoing constant topographic changes. Observation of specific topographic deformations in these areas are of great importance for coastal maintenance and research. The long-term development of the coast is closely followed by the establishment and analysis of so-called coastal state indicators (CSI). Examples are the width of the beach and dune volume (Davidson *et al.*, 2007; Van Koningsveld *et al.*, 2005). The importance to quantify beach width and derive optimal/acceptable values for coastal management was stressed by (Tucker *et al.*, 2019). Also, the long-term development of beach width has been related to dune evolution (Galiforni Silva *et al.*, 2019).

Different types of data are used to quantify these CSIs. Observations range from satellite data (large scale, medium to high temporal frequency) to in-situ measurements (small scale, local, low temporal frequency/incidental). In the middle of this spectrum lays permanent laser scanning (PLS). PLS makes use of a permanently installed programmable laser scanner to observe small-scale changes (theoretically up to cm range) at high temporal frequency (up to hourly). The changes in CSIs discussed in this article are in the range of several decimetres to meter due to lower point spacing at the edges of the point clouds and high variability of the shoreline due to waves.

The resulting data set contains a large number of consecutive point clouds and thus provides a 3D representation of a section of the coast and its evolution over time. This source of information on deformations and processes is comprehensive, but the analysis of CSIs is not immediate. The subject of this research is to make information on the evolution of the coast from PLS data accessible in the form of coastal state indicators.

B. *Research Questions*

In this work we are analysing the possibilities to estimate two coastal state indicators that give indications on the development of a sandy beach with permanent laser scanning, by answering the following research questions:

1. How can the width of the beach be detected automatically from laser scanning point clouds?
2. How can we detect the separation between dry beach and intertidal area?
3. How do extreme weather conditions influence these parameters?

To answer these questions, we derive digital elevation models, estimate the extent of the point clouds and locate the approximate shoreline at high tide and low tide per month.

C. *Related Work*

Beach width is mentioned by (Van Koningsveld *et al.*, 2005) as a coastal state indicator, relevant for coastal management as recreational factor as well as for disaster prevention. Optimal values for recreational use were derived by (Tucker *et al.*, 2019). Definition of coastal state indicators and the observation of the coast with regular imaging from fixed positions have been studied for example by (Davidson *et al.*, 2007). Additional studies deriving coastal state indicators for the Dutch coast have been presented by (Giardino *et al.*, 2014) and (Jimenez *et al*., 2007). The latter derived automatic methods to estimate beach visitor distribution from video images of the beach. Also, CSIs are an important tool for the Dutch Ministry of Infrastructure and Water Management to make decisions about coastal management, for example about the necessity and quantity of beach nourishments.

A long-term study on monitoring the position of the shoreline with the help of laser scanning data was performed by (Caudle *et al.*, 2019) for a part of the Texan coast in the US over a period of 13 years. (Castelle *et al.*, 2021) presented a method to monitor the long-term development of the shoreline on a part of the French coast from satellite data. Next to satellite image data they made use of wave and tide hindcast data to limit the considerable uncertainty that resulted from large tidal ranges and relatively low-resolution satellite images. Beach width is estimated from yearly JARKUS data by (Keijsers *et al.*, 2014) and related to dune development by (Galiforni Silva *et al.,* 2019). The study of (Van IJsendoorn *et al*. 2021) makes use of JARKUS data to quantify dune growth and relates it to sea level rise.

A study of the set-up of a permanent laser scanner with the same equipment as used for this research was presented by (Vos *et al*., 2022). The resulting data set has subsequently been analysed to detect 4D objects of change (Anders *et al*., 2020), and change pattern with the help of k-means clustering (Kuschnerus *et al*., 2021). The latter resulted in a separation between a cluster dominated by erosion in the intertidal area and a relatively stable cluster on the dry part of the beach.

D. *Data Set*

The data set used for this research is a selection of 3D point clouds out of an hourly data set covering two years of permanent laser scanning. The data set is acquired with a RieglVZ-2000 laser scanner mounted on the balcony of Grand Hotel Huis ter Duin in Noordwijk, The Netherlands. It is overlooking a section of the coast, including an about 1km long part of dunes and beach. The coast consists of dunes and a sandy beach that is varying in size (width and height) depending on tides, wave heights and weather conditions and human (maintenance) activities.

Our study covers the period of 1st January 2020 until end of April 2020. This period includes three major storms, on 9/10 February, 17/18 February, and 22/23 February 2020.

Each point of the point cloud is represented by 3D coordinates (x,y,z-coordinates). For each point cloud the respective inclination angles (pitch and roll) of the laser scanner at the time are recorded by the internal inclination sensors of the laser scanner. These angles are used to correct each point cloud for small deviations due to changes in the tilt and orientation of the laser scanner.

We make use of tide data consisting of hourly measured water levels above NAP, collected and distributed by the Dutch Ministry of Infrastructure and Water Management (Rijkswaterstaat, 2022) at Scheveningen, a coastal city about 20 km south of Noordwijk.

II. Methods

The methods are presented in three parts. First, we explain the pre-processing steps that we take to prepare the data set, then we present two different methods to derive the beach width and the width of the intertidal area.

A. *Pre-processing*

In a first step we loop through each point cloud of the four-months data set, get the inclination values and align the data with a simple rotation matrix based on the pitch and roll values per scan. Then we remove all points with z-coordinates larger than 20 m and x-coordinates larger than -100 m, as they are not part of the beach. Of this reduced point cloud, we generate a digital elevation model (DEM) with 1 m x 1 m regular grid parallel to the coastline taking the mean elevation of all grid cells that contain at least one point (for an overview see Figure 1).

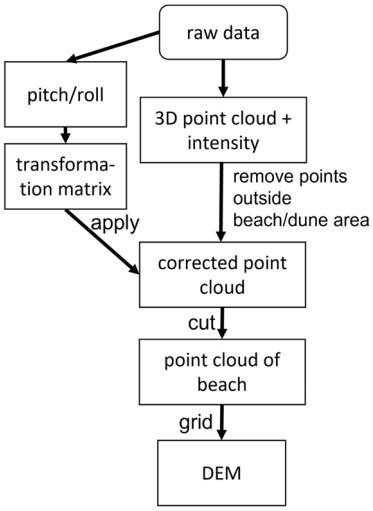

Figure 1. Schematic of pre-processing steps from raw data to DEM applied to each individual point cloud.

B. *Estimating Beach Width and Intertidal Width directly from DEMs*

The waterfront is roughly perpendicular to the 0°-scan-line (see Figure 2). Further, we assume that the dune foot is constant throughout our observation period at an x-coordinate of about -145 m in the local coordinate system of the laser scanner (see Figure 2). The exact location of the border between the dunes and the beach is not covered by our data set, due to the dunes blocking the sight of the dune foot.

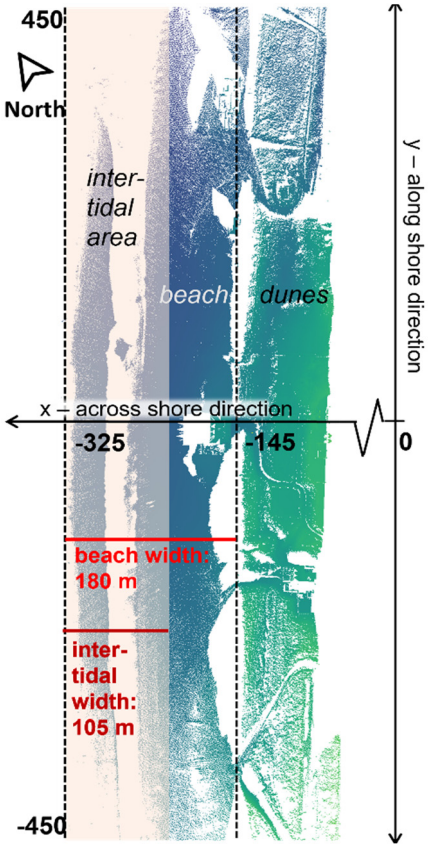

Figure 2. Point cloud of beach and dunes in Noordwijk on 01-01-2020 at 15:00, coloured with elevation. The estimated width of the beach and width of the intertidal area are shown as an example.

We define the sandy beach as the part of the beach that is more than 145 m (approximate location of the dune foot) away from the laser scanner, which means, all points of the point clouds with x-coordinate smaller than -145. The observed part of the beach is limited by the range of the laser scanner, and we discard areas with very low point density. We consider the area within 450 m along shore to the North and South of the laser scanner (*i.e.*, all points with y-coordinate: - 450 <= y <= 450). The dry part of the beach is the sandy beach that is never covered by high tides and therefore mostly dry, unless it is raining. The width of the beach is the distance in x-direction between the dune foot (estimated to be at -145 m in local scanner coordinate system) and the point on the beach with the lowest x-coordinate at the lowest water level during one day. This means that the beach width is determined only by the variability of the water height. The most seawards border between the water and the sandy beach at that time is the shoreline at low tide.

The shoreline at high tide is the line between water and sandy beach at the highest water level per day. The area between the low tide shoreline and the high tide shoreline is what we call the intertidal area in this article. The width of the intertidal area is the across shore distance between the highest point of the high tide shoreline and the lowest point of the low tide shoreline (see Figure 2 for an illustration).

To estimate the width of the beach and the width of the intertidal area, as well as the approximate location of the high tide shoreline, we remove all columns of the DEM with less than ten non-empty grid cells. Then we extract the lowest x-coordinate from each generated DEM. We save this minimal x-coordinate per DEM and find the smallest minimal x-coordinate and the largest minimal x-coordinate per day and save the times at which they occurred. This provides an estimate of the times of low and high tide.

By subtracting the smallest minimal x-coordinate from the location of the dune foot, we get the estimated beach width for that day. Deriving the difference between this value and the largest minimal x-coordinate per day we get an estimated width of the intertidal area. Both estimated widths are in meters resolution because of the size of the grid cells of the DEM.

To filter the results for the most reliable values, we check if the estimated smallest beach width per day and largest beach width per day match the actual low and high tides. We compare the times that the respective point clouds were taken with the tide data from (Rijkswaterstaat, 2022). If these times roughly match, *i.e.* agree within a threshold of two hours, we assume that the estimated beach width is close to the actual width of the beach at the lowest water level on that day. If the times disagree, we discard the beach width for that day. Subsequently we use the remaining points to calculate the average width of the beach and average width of the intertidal area per month.

C. *Estimating Shoreline at High and Low Tide*

As an alternative method we use the data from Rijkswaterstaat to select the point cloud that resulted from a scan closest to the time of highest tide and lowest tide per day. From this selection of point clouds, we generate DEMs as described above and get the location of the shoreline as the grid cells that are at the border of the DEM in x-direction. This provides two shorelines per day, one at high tide and one at low tide. Each shoreline is then filtered for extreme outliers.

We collect all shorelines at high tide for one month and take the most landwards point for each alongshore position to derive the high tide shoreline of that month. From all shorelines at low tide, we use the most seaward point for each alongshore location to derive the low tide shoreline of that month. Then we fit a second-degree polynomial to both of these shorelines and estimate the beach width and the width of the intertidal area per month from the extremum of the fitted curves.

III. Results

The results are presented in three parts. We first analyse the estimated width of the beach and the intertidal area from the direct method. Then we present the results of the estimation of the shorelines and subsequently we compare both methods over the entire period of January to April 2020.

A. *Estimation of Beach Width*

The beach width was estimated for January and February 2020 as described above and is shown in Figure 3. The beach width is varying between 150 m and 250 m and the width of the intertidal area between 50 m and 180 m for most days. The estimated times of high tide and low tide match the times from the tide data of Rijkswaterstaat on 24 days in a two-months period. This indicates that our method to find the point cloud with the largest extend of the beach is not optimal, and most likely misrepresents the estimated widths in 60 % of the cases. It can be seen clearly that the width of beach and intertidal area both vary more in February than in January.

There are many factors that influence the extend of a point cloud next to the actual water height. Weather conditions such as heavy rain and low visibility due to fog can reduce the size of the visible part of the beach. Figure 4 shows a point cloud at high tide during a storm in February 2020, we can see the large number of points resulting from reflections of the high waves.

To further investigate reasons for inaccurate beach width estimations, we plot all the high tide shorelines and all the low tide shorelines for January 2020 as shown in Figures 5 and 6. It can be seen clearly in Figure 5 that reflections from high waves especially during high tides are mistaken for parts of the beach, disturbing the estimated low tide shoreline.

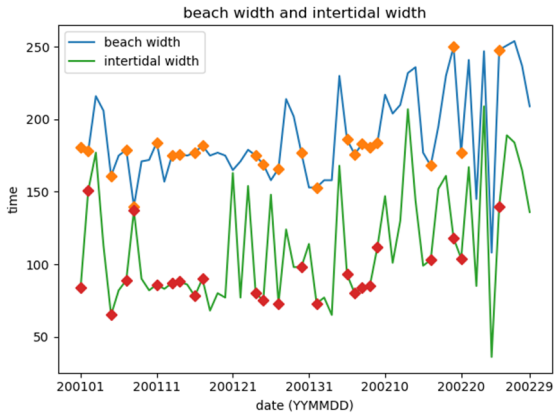

Figure 3. Width of the beach and the intertidal area estimated from the largest and smallest point clouds per day. The estimates where both high tide and low tide matches the time of the tide data from Rijkswaterstaat are marked with a diamond.

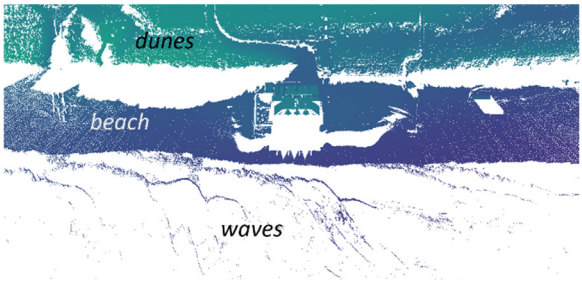

Figure 4. Point cloud at high tide on 10-02-2020 during a heavy storm. A large part of the beach is covered with water. Reflection of the waves can clearly be seen.

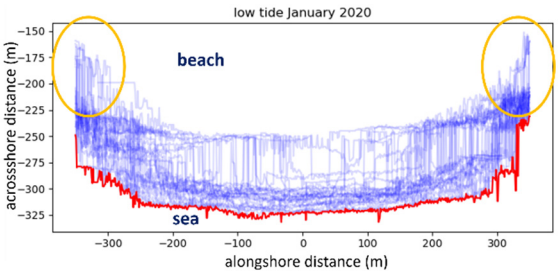

Figure 5. All estimated shorelines at high tide in January 2020 with the minimum of all lines marked in red. The outliers due to high waves are circled yellow.

In Figure 6 we clearly see the effects of the lower point density with increasing range around 400 m. This leads to an artificial border of the point cloud that is mistaken as part of the low tide shoreline.

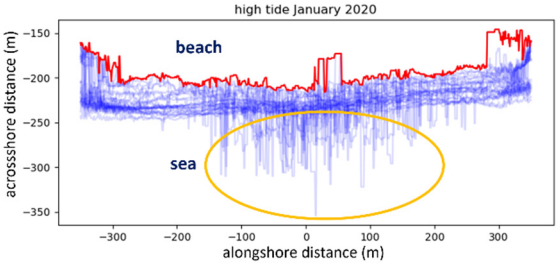

Figure 6. All estimated shorelines at low tide in January 2020 with the minimum of all lines marked in red. The areas circled in yellow show the effect of reduced point density in the point cloud around 400 m range.

B. *Comparison*

We fit a curve (2nd degree polynomial) through the high and low tide shorelines and use the local minimum of this curve to derive an alternative estimate for the monthly beach and intertidal width. These are shown for January and February 2020 in Figures 7 and 8.

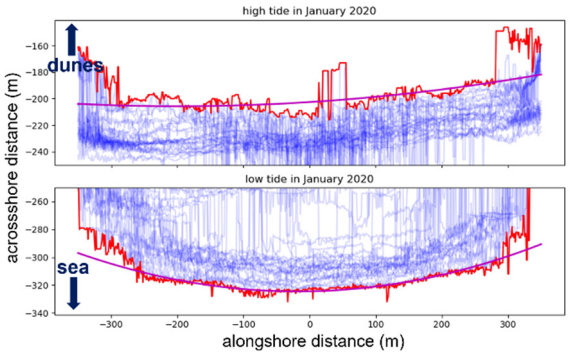

Figure 7. Curve (in purple) fitted through minimal low tide shoreline and maximal high tide shoreline for the estimation of beach width and intertidal width in January 2020.

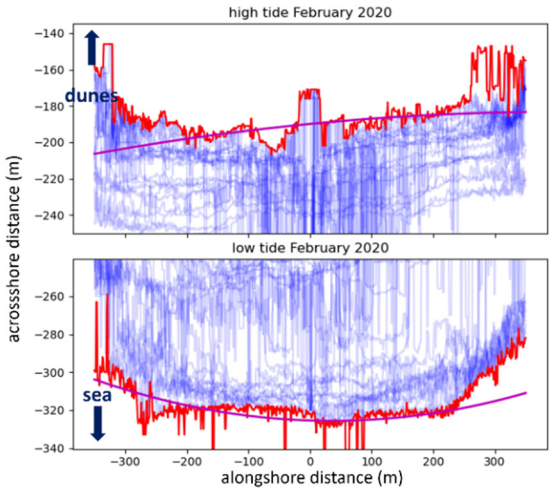

Figure 8. Curve (in purple) fitted through minimal low tide shoreline and maximal high tide shoreline for the estimation of beach width and intertidal width in February 2020.

From the estimated width as presented in Section III A, the average beach width in January 2020 is 173 m and the estimated width of the intertidal area is 92 m. From the high and low tide shorelines shown in Figure 7 we estimate the total beach width for January 2020 around 179 m and the width of the intertidal area 119 m.

For February 2020 we estimated an average beach width of 191 m, considerably larger than in January and an intertidal width of 99 m. With the high and low tide shorelines as shown in Figure 8 we derive a beach width of 180 m and an intertidal width of 137 m. We can clearly see the effect of the extreme weather here. If we take the extend of all the shorelines as an indication for the uncertainty of the monthly shoreline, there is a much higher uncertainty in February than in January. Both high and low tide shoreline are varying much more and cannot be distinguished as easily from their location on the beach alone.

As shown in Table 1, the width estimated by both methods do not match for every month. Note that the width of the intertidal area is considerably smaller in March and April than in January and February, which we attribute to the extreme stormy weather conditions, especially in February.

Table 1. Table with estimated beach width and intertidal width from two different methods

Month	Width estimated directly from point clouds [m]		Width estimated from high and low tide shorelines	
	Beach	Intertidal	Beach	Intertidal
January 2020	173	92	179	119
February 2020	191	99	180	137
March 2020	190	103	196	141
April 2020	197	97	191	116

IV. Discussion

We present two different methods to estimate the width of the beach directly form DEMs from point clouds from PLS, by evaluating the maximal width of smallest and largest point cloud per day as well as by extracting the location of the high and low tide shoreline and comparing these.

Both methods have their draw backs. They often mistake reflections from high waves, especially at high tide, as parts of the beach leading to overestimated width, or unrealistic peaks in the high and low tide shorelines. Additionally, weather conditions like dense fog or heavy rain, limit the extend of the point clouds and therefore lead to erroneous estimations. Overall, the method of first estimating high and low tide shorelines appears more reliable than the 'direct' method. Additional smoothing/filtering applied to the high and low tide shorelines could even further improve the results. Further, filtering the lines with too many outliers will lead to additional improvement.

Another way to validate our estimations of beach width, is the comparison with estimations from camera images. This validation is part of the ongoing research and will be presented in future publications.

The z-coordinate or elevation of the minimal x-coordinate and the entire high and low tide shorelines has not been considered for this research. Including this additional information, could potentially improve the beach width estimation, as well as deliver more insights into the coastal change detection. The estimation of beach runup due to waves and wind setup is another open question to be considered during future analysis of the PLS data set.

As presented by (Kuschnerus *et al.*, 2021) a clustering approach was used on the time series derived from daily point clouds for a similar dataset of the coast in Kijkduin, The Netherlands. This method was applied here as well, as an example for the month of January (see Figure 9). The resulting clusters can be used to find

the border between eroding and accreting areas, which roughly corresponds with the location of the high water line. Therefore, this method, with some more refinement can potentially provide another alternative to derive the beach and intertidal width and compare with the methods presented here.

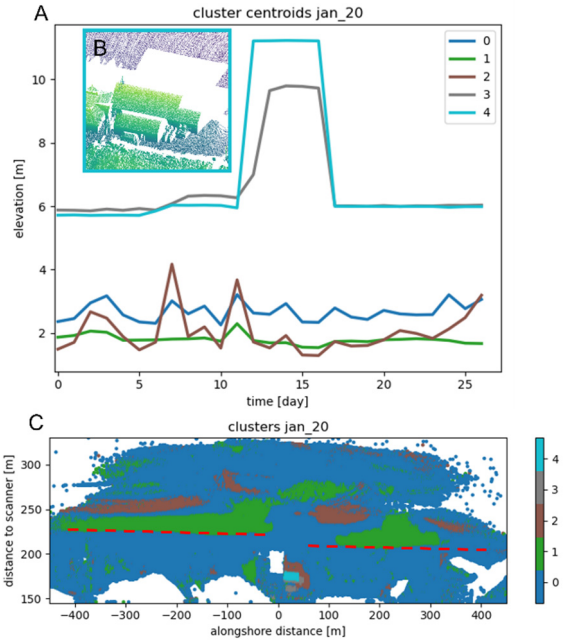

Figure 9. k-means clustering for January 2020. A: Mean time series per cluster, with peak in clusters 3 and 4, caused by tents. B: Point cloud with tents. C: Point cloud coloured by cluster with estimated border between dry beach and intertidal area shown as dashed line in red.

V. Conclusion

This research presents the estimation of two CSIs: beach width and intertidal width from PLS data, to quantify the deformation of a typical coastal beach in The Netherlands. We derived two methods to estimate both CSIs from DEMs of the 4D point cloud data set. High waves and other extreme weather conditions, like fog and heavy rain lead to inexact estimations of both beach width and intertidal width. However, when considering the results for the entire month, we obtain valid estimates varying between 173 m and 197 m (beach width) and between 92 m and 141 m (intertidal width). The heavy storms in February influence the uncertainty of the estimation and render it less reliable. Future research will include the estimation of wave runup and make use of the elevation of the shorelines to improve the estimates for beach width and intertidal width, as well as the entire coastal deformation. A possible extension of this research is the inclusion of the clustering of time series from PLS data. Ultimately, the quantification of CSIs from PLS data at high temporal frequency (monthly) and with high spatial accuracy (meters) will improve understanding of coastal deformation and support coastal management.

VI. Acknowledgements

The authors would like to thank Grand Hotel Huis ter Duin for their cooperation. This research has been supported by the Netherlands Organization for Scientific Research (NWO, grant no. 16352) as part of the Open Technology Programme and by Rijkswaterstaat (Dutch Ministry of Infrastructure and Water Management).

References

Anders, K., Winiwarter, L., Lindenbergh, R., Williams, J.G., Vos, S.E., and Höfle, B. (2020). 4D objects-by-change: Spatiotemporal segmentation of geomorphic surface change from LiDAR time series. *ISPRS Journal of Photogrammetry and Remote Sensing*, 159, pp. 352–363.

Castelle, B., Masselink, G., Scott, T., Stokes, C., Konstantinou, A., Marieu, V., and Bujan, S. (2021). Satellite-derived shoreline detection at a high-energy meso-macrotidal beach. *Geomorphology* 107707.

Caudle, T.L., Paine, J.G., Andrews, J.R., and Saylam, K. (2019). Beach, Dune, and Nearshore Analysis of Southern Texas Gulf Coast Using Chiroptera LIDAR and Imaging System. *Journal of Coastal Research* 35, pp. 251–268

Davidson, M., Van Koningsveld, M., de Kruif, A., Rawson, J., Holman, R., Lamberti, A., Medina, R., Kroon, A., and Aarninkhof, S. (2007). The CoastView project: Developing video-derived Coastal State Indicators in support of coastal zone management. Coastal Engineering. *The CoastView Project: Developing coastal video monitoring systems in support of coastal zone management* 54, pp. 463–475.

Galiforni Silva, F., Wijnberg, K.M., de Groot, A.V., and Hulscher, S.J.M.H. (2019). The effects of beach width variability on coastal dune development at decadal scales. *Geomorphology* 329, pp. 58–69.

Giardino, A., Santinelli, G., and Vuik, V. (2014). Coastal state indicators to assess the morphological development of the Holland coast due to natural and anthropogenic pressure factors. *Ocean & Coastal Management* 87, pp. 93–101.

Jiménez, J.A., Osorio, A., Marino-Tapia, I., Davidson, M., Medina, R., Kroon, A., Archetti, R., Ciavola, P., and Aarnikhof, S.G.J. (2007). Beach recreation planning using video-derived coastal state indicators. Coastal Engineering. *The CoastView Project: Developing coastal video monitoring systems in support of coastal zone management* 54, pp. 507–521.

Keijsers, J. G. S., Poortinga, A., Riksen, M. J. P. M., and Maroulis, J. (2014). Spatio-Temporal Variability in Accretion and Erosion of Coastal Foredunes in the Netherlands: Regional Climate and Local Topography. *PLOS ONE* 9, e91115 (2014).

Kuschnerus, M., Lindenbergh, R., and Vos, S. (2021). Coastal change patterns from time series clustering of permanent laser scan data. *Earth Surface Dynamics*, 9(1), pp. 89–103.

Rijkswaterstaat, (2022). Dutch Ministry of Infrastructure and Water management. Available in url: https://www.rijkswaterstaat.nl/water/waterdata-en-waterberichtgeving/waterdata/getij

Tucker, T.A., Carley, J.T., Couriel, E.D., Phillips, M.S., and Leaman, C.K. (2019). Seawalls and acceptable beach width for public amenity. *Australasian Coasts and Ports 2019*

Conference: Future directions from 40 [degrees] S and beyond, Hobart, 10-13 September 2019, 1158.

Van IJzendoorn, C. O., de Vries, S., Hallin, C., and Hesp, P. A. (2021). Sea level rise outpaced by vertical dune toe translation on prograding coasts. *Sci Rep* 11, 12792.

Van Koningsveld, M., Davidson, M.A., and Huntley, D.A. (2005). Matching Science with Coastal Management Needs: The Search for Appropriate Coastal State Indicators. *Journal of Coastal Research* pp. 399–411.

Vos, S., Anders, K., Kuschnerus, M., Lindenbergh, R., Höfle, B., Aarninkhof, S., and de Vries, S. (2022). A high-resolution 4D terrestrial laser scan dataset of the Kijkduin beach-dune system, *The Netherlands. Sci Data* 9, 191.